JOURNAL OF AIRCRAFT
Vol. 45, No. 4, July–August 2008

Application of Piezoelectric Actuators at Subsonic Speeds

M. Amir*
University of Southampton, Southampton, England SO17 1BJ, United Kingdom
and
K. Kontis†
University of Manchester, Manchester, England M60 1QD, United Kingdom

DOI: 10.2514/1.35630

An experimental study has been conducted to investigate the effects of using a series of piezoelectric actuators at two chordwise positions (25 and 50% chord length) on a NACA 0015 aerofoil at subsonic speeds. The lift and drag forces were measured using a three-component force balance. A detailed boundary-layer survey was carried out using hot-wire anemometry. The actuators operating at 25% chord length are more effective, resulting in an increase of the lift-to-drag ratios at higher frequencies. Boundary-layer surveys indicated that, with the actuators operating at 25% chord length, the boundary-layer thickness is drastically reduced downstream of their location, whereas the flow remains mostly undisturbed in the upstream direction. The actuators can fix laminar to turbulent transition and eliminate the laminar separation bubble at lower Reynolds numbers.

Nomenclature

$0.25c$	=	25% chord length
$0.5c$	=	50% chord length
c	=	chord length of the aerofoil
C_d	=	drag coefficient
C_ℓ	=	lift coefficient
$C_{\ell\,\max}$	=	maximum lift coefficient
C_ℓ/C_d	=	lift-to-drag ratio
d	=	drag force
ℓ	=	lift force
Re_N	=	Reynolds number
$U_{\rm rms}$	=	root mean square velocity
U_∞	=	freestream velocity
$U_{\rm rms}/U_\infty$	=	turbulence intensity
U_0	=	velocity at the edge of the boundary layer
y	=	vertical distance above the aerofoil
α	=	angle of attack
δ	=	boundary-layer thickness
δ^*	=	displacement thickness
θ	=	momentum thickness

I. Introduction

IN THE last century, increased attention has been devoted to the development of techniques capable of enhancing our ability to control unsteady flows in a wide variety of configurations. Controlling the flow in and around them can lead to greatly improved efficiency and performance. It involves the manipulation of the boundary-layer separation, which is associated with large energy losses and in most applications unfavorably affects the aerodynamic loads in the form of lift loss and drag increase. Hence, there is a strong motivation to manipulate or delay the occurrence of flow separation in systems involving fluid flow such as in air (aeroplane wings), land, or underwater vehicles as well as in turbomachines and diffusers. Prandtl [1] developed the boundary-layer theory concept in 1904. From that period onward, the revolutionary work of Schubauer and Skramstad on steady-state tools and mechanisms for flow management produced the foundation for flow control. Recently, a comprehensive review and analysis were made by Gad-el-Hak and Bushnell [2].

Flow control involves active [3–5] or passive devices [6,7] with useful end results including drag reduction, lift enhancement, mixing augmentation, and flow-induced noise suppression. Active flow control is a multidisciplinary research area combining sensing, actuation, flow physics, and control with the objective of modifying flowfield characteristics to achieve a desired aerodynamic performance. Unlike passive techniques, such as geometric shaping to adjust the gradient pressure or placement of longitudinal grooves or riblets on a surface to reduce drag, active control manipulates a flowfield by using a time-dependent forcing system, typically to leverage a natural instability of the flow and thus to amplify the control effectiveness. Advantages of active flow control include the ability to attain a large effect using a small, localized energy input and to control complex dynamical processes, for example, the reduction of skin friction and hence viscous drag [8,9] in turbulent boundary layers.

Piezoelectric materials such as lead zirconate titanate ceramics when subjected to an electric field produce mechanical strain or alternately generate an electric charge when subjected to a mechanical strain. This property gives piezoelectric materials the ability to act as actuators or sensors. The concept of using piezoelectric actuators in devices that alter the way in which an aerofoil interacts with its environment is not new. In fact, several notable research institutions, federal laboratories, and industrial partners are actively pursuing this type of research. The main driving force for this activity is increased fuel economy, lighter aircraft, and the elimination of hydraulically actuated control surfaces. One of the areas that incorporates the use of these materials is the area of active noise and vibration control [10–12]. Piezoelectric actuators were first used for flow control by Wehrmann in the mid-1960s [13–15]. However, their utility in practical situations was limited as a result of the reduction in their response far from their natural frequency. Wiltse and Glezer devised a clever excitation scheme that employed the amplitude modulation of a resonant carrier waveform [16]. Their technique allowed for the effective excitation of free-shear flows away from the natural frequency of the actuators. Jacobson and Reynolds have also recently applied this technique to wall-bounded flows [17]. During the past decade, piezoelectric actuators as the active element in synthetic jets demonstrated that they could significantly enhance the overall lift of an aerofoil. Synthetic jets have also been proven to be an effective tool for reducing drag and

Received 12 November 2007; revision received 15 January 2008; accepted for publication 16 January 2008.

*Research Fellow, School of Engineering Sciences.
†Senior Lecturer, Head of Aerospace Research Group and Aero-Physics Laboratory, School of Mechanical, Aerospace and Civil Engineering; k.kontis@manchester.ac.uk. Senior Member AIAA.

enhancing mixing [18]. Synthetic jet systems have been produced with speakers, compressed air, air pumps, and bimorph diaphragms. All of these techniques add weight, require real estate, and add complexity to an aeroplane, making these options impractical. Piezoelectric actuators are an attractive solution because of their light weight and fast time response; they have no contacts, they are highly reliable, and most importantly they are cheap to produce. Sinha [19] developed a flexible composite surface (FCS), which could be affixed to the surfaces of aircraft wings to reduce profile drag. Even though the FCS is a thin passive device, it modifies the wall-normal velocity profile and pressure gradient in the device neighborhood in the same way a piezoelectric actuator does. From the results, drag reductions of 18–37% were observed in flight tests on light aircraft and sailplanes. The FCS interacted with the nonzero pressure-gradient boundary layer through submicron-level flexural vibrations. The interaction of the FCS flow-wall surface damped out turbulent fluctuations at all but a selected frequency. The resulting modified boundary layer displayed resistance to separation similar to turbulent flows while offering the low skin-friction characteristics of laminar boundary layers. The FCS was believed to encourage the formation of streamwise vortices. Such vortices enhanced the attachment of the thin wall layer. The FCS also prevented the formation of a laminar separation bubble on the nonlaminar flow wing of the Standard Cirrus. Drag reduction was also observed over the entire range of airspeeds.

Mangla and Sinha [20] used a leading-edge-mounted active flexible wall (AFW) transducer to interact with unsteady separating boundary layers over a sinusoidally pitching NACA 0012 aerofoil. The AFW transducer consisted of a metallized Mylar membrane stretched across an array of thin-strip-shaped high and low electrodes. The ac actuation at the optimum actuation frequencies produced membrane vibrations around 0.01 μm amplitude over the actuated strips. The optimum vibration frequencies resulted in a strip spacing and local freestream velocity based Strouhal number of 1 and delayed the onset of dynamic stall by about 2 deg. AFW actuation at the point of zero pressure gradient before separation also lowered the prestall lift and moment coefficients. However, an improper actuation location advanced the dynamic stall. In general, drastic changes in pressure at the leading edge, around the point of zero pressure gradient, were found on the suction side.

Choi et al. [21] conducted experiments to control the flow around an aerofoil using piezoceramic actuators. The actuator was made of spring steel on which a unimorph piezoceramic material sheet was bonded. Seven actuators were mounted along the span of the suction surface with a 2-mm gap between adjacent actuators. Lift and pitching moment coefficients were obtained in the absence of the actuators. These were compared with those obtained with and without control (the actuator on and off conditions, respectively). At low angles of attack, the lift coefficients for the cases of the actuator on and off were smaller than that for the case of no actuator. At high angles of attack, the actuation increased C_ℓ. The stall angle was increased by about 2 deg due to control, as compared with the case with no actuators. The maximum lift coefficient was also increased by 10 and 17%, respectively, as compared with the cases of the actuator off and no actuator. The quarter-chord pitching moment coefficient became nearly zero with the actuators at all of the angles of attack investigated, whereas it was negative at high angles of attack without the actuators. The changes in the flowfield due to control were also studied using flow visualization at a 15 deg incidence. With the actuators off, the streak lines showed that separation occurs downstream of the location of the actuators, whereas an attached flow was observed with the actuators on, indicating the delay of separation due to control. Their study, therefore, showed that the flap-type piezoceramic actuators attached to the aerofoil suction surface effectively increased the lift force at higher angles of attack by delaying separation.

Although Choi et al. [21] conducted a similar investigation to the present study, no previous work has examined the effect of actuators on the boundary layer at various Reynolds numbers. The current work investigates the changes in the boundary-layer characteristics at a number of angles of attack and the effect of varying the Reynolds number. It aims to shed light onto the physical mechanisms associated with the operation of the actuators. In addition to this, it also investigates their effectiveness at two different chordwise positions on a NACA 0015 aerofoil. The effect of driving frequencies and the freestream Reynolds number (Re_N) on the aerodynamic characteristics (such as lift and drag forces) is also reported.

II. Experimental Setup and Apparatus

The experiments were conducted in a low-speed subsonic wind tunnel. The tunnel has a test section of 1400 (length) $\times$ 450 (width) $\times$ 450 mm (height). The floor is made of medium density fiber wood. The ceiling and side walls are made of high-transparency perspex to allow optical access for photography and visualization. The contraction ratio of the nozzle is 6.5 to 1, and the maximum velocity of the test section is 32 m/s. Measurements were taken at a Re_N of 280,000 and 480,000 based on the freestream velocities of 16 and 28 m/s. The freestream turbulent intensity of the tunnel is less than 0.15%. The wind tunnel was fitted with a top-mounted three-component force balance.

The balance rod holds the aerofoil in position about the 25% chord point. The model support was free to rotate in the force plate for the adjustment of the angle of attack of the model, whereas its position was locked by means of an incidence clamp. The forces on the aerofoil were transmitted by way of flexible cables to strain gauge load cells, which measure the fore and aft lift forces and the drag force. The output from each load cell was taken to a strain gauge amplifier carried on the mounting plate and via a flexible cable. The two lift cables that acted horizontally in this configuration had to be counteracted by an optimum weight, which gave the desired range of aft and fore outputs of the lift component.

The aerofoil was rectangular in shape and had a constant symmetric NACA 0015 aerofoil section. It had a 0.25-m chord and a span of 0.455 m. The maximum thickness was 0.0375 m. Two chordwise positions were chosen to place the piezoelectric diaphragms along its span, one at 25% chord ($0.25c$) and the other at 50% chord ($0.5c$). Figure 1 shows an isometric view of the aerofoil.

For the purpose of the present work, the piezoelectric diaphragms used in the test were MENA 7BB-41-2A0, manufactured by MuRata Electronics North America, Inc. Figure 2 shows the material type and dimensions of the diaphragm.

According to the manufacturer, the piezoelectric diaphragm undergoes vibrations of very small amplitudes (less than 0.1 mm). The factors affecting the amplitude of the vibrations are 1) the supplied voltage, 2) the frequency of operation, and 3) the method of mounting the diaphragms.

The amplitude of the vibration increases only very slightly with frequency [22]. At the resonant frequency of the diaphragm, maximum amplitude is achieved. Increasing the frequency beyond the resonant value decreases the amplitude of the vibration of the diaphragm. Investigations have also been carried out in [22] on the maximum amplitude of the diaphragms when mounted by different

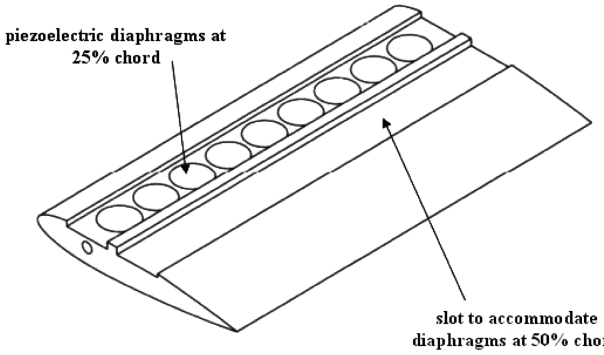

Fig. 1 NACA 0015 aerofoil showing the actuators placed on its upper surface.

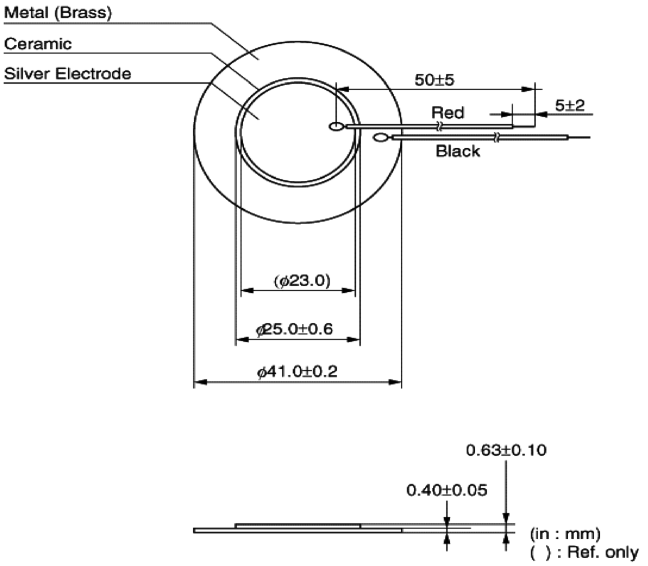

Fig. 2 Specifications of the piezoelectric actuator.

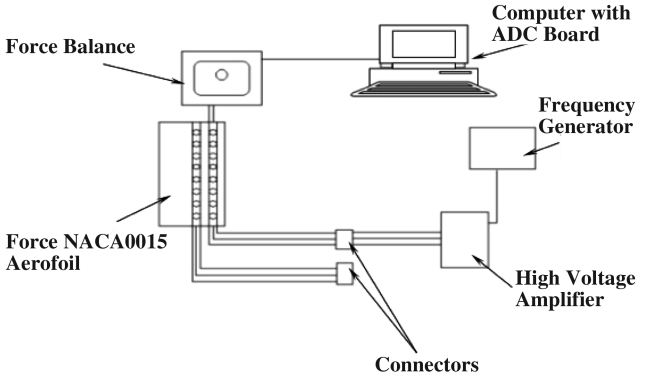

Fig. 3 Schematic of the data acquisition system.

methods. However, in the current study, only one suitable method of mounting the diaphragms was chosen. Circular slots were created using CNC Machining on each slot to accommodate the diaphragms. The diaphragms in this study were glued on the surface using Araldite super glue. The empty slots were covered with a filler to ensure a smooth, flush surface.

Fiber optic displacement sensors [22–24] have been used to measure the diaphragm center displacements. Preliminary tests were conducted to examine the range of operational frequencies of the actuators using the current mounting method. A simple analogue displacement sensor was placed on top of the actuator just touching its surface to measure the amplitude of oscillation at different frequencies. The results indicated that, outside the 200–1000 Hz envelope, the amplitude was negligible. Based on this observation, three representative frequencies were selected, that is, 300, 500, and 900 Hz.

The piezoelectric diaphragms were connected in parallel to the voltage source via a high-voltage amplifier. This was to ensure equal voltage distribution among the diaphragms. A frequency generator was connected to the amplifier to alter their frequencies of operation. A computer with a National Instrument data acquisition system was used to capture the data. To record the mean aerodynamic forces, a sampling rate of 2 kHz was used over 2 s. The estimated overall accuracy for the force measurements (i.e., the lift and drag forces) was $\pm 5\%$. The percentage error in the estimation of C_ℓ, C_d, and C_ℓ/C_d due to the uncertainty in the velocity measurement and mounting of the force balance was ± 7, 8, and 10%, respectively.

A single component hot-wire anemometry was used to determine the mean velocity and turbulent intensity profiles. A static calibration of the hot wire, based on King's law, was obtained by placing the probe in the freestream at the beginning of the working section.

The hot wire was also calibrated in the freestream against a Pitot static tube before and after the experiments to avoid drifting due to ambient temperature variations or other factors. The error in the velocity reading was approximately $\pm 2.5\%$. Measurements were taken at six different chordwise positions, $x/c = 0.15$, 0.25, 0.35, 0.55, 0.75, and 0.95, and at a sampling rate of 1 kHz over a period of 4 s. Figure 3 shows a schematic of the data acquisition system.

Wind tunnels are used to test the aerodynamic characteristics of aircraft, and the influence of the tunnel walls must be taken into account when considering test results. Historically, wind-tunnel corrections have been based on linear potential flow theory [25]. To obtain good quality and reliable test data, factors relating to wall interference, flow angularity, local variations in velocity, and support interference must be taken into account. In the current study, the equations used for the wind-tunnel interference and the blockage corrections were obtained from Engineering Sciences Data Unit data sheets [26]. The interference and blockage factors that were used apply to a two-dimensional aerofoil (the NACA 0015 aerofoil in this case) spanning and centrally placed in a rectangular wind tunnel with closed and solid side walls. Based on the blockage factors, the corrections in the lift and drag coefficients were made using the equations given in [26]. The values were then calculated by adding the corrections to the measured values.

III. Results and Discussion

A. Force Measurements

The measurements were taken with the "actuators off" (i.e., when the actuators were not electrically simulated), and these were then compared with the "actuators on" (i.e., when the actuators were electrically simulated) at three different frequencies: 300, 500, and 900 Hz. The effect of the Re_N was also examined on the forces acting on the aerofoil. The measurements were taken at a low Re_N of 280,000 and a high Re_N of 480,000. The effect of the piezoelectric actuators was first examined at $0.25c$ and then at $0.5c$.

1. *Actuators Operating at* $0.25c$

Figure 4a shows that, with the actuators operating at a Re_N of 280,000, there seems to be no considerable effect on C_ℓ. However, there is a slight decrease in C_ℓ between 9 and 14 deg. The maximum lift coefficient ($C_{\ell\max}$) occurs at an incidence of 17 deg with the actuators off. This value slightly decreases with the actuators on for all of the frequencies tested. However, at a Re_N of 480,000, a considerable increase in C_ℓ is evident in Fig. 4b. Unlike at a low Re_N, the positive effect of the actuators on C_ℓ can be seen from low incidence (i.e., 3 deg) to the poststall conditions. $C_{\ell\max}$ is also increased at a higher Re_N. Also, at a low Re_N, actuators operating at 300 Hz seem to alter C_ℓ slightly more than those operating at higher frequencies. However, at a high Re_N, there seems to be no effect of increasing the frequency of the actuators on C_ℓ. The effect of Re_N on the performance of the actuators is, therefore, evident in Fig. 4.

Figure 5 shows the variation of the drag coefficient (C_d) against α. Figure 5a shows that, at a Re_N of 280,000, C_d seems to increase due to the actuators. This effect is seen at all incidences. Previously, Fig. 4a showed a slight decrease in C_ℓ as well, at the same Re_N. This suggests that at a low Re_N, there is a negative effect of the piezoelectric actuators on both C_ℓ and C_d. When the Re_N is increased to 480,000, the effect of altering the frequency of the actuators is evident in Fig. 5b. At 300 and 500 Hz, C_d seems to increase, whereas, with the actuators operating at 900 Hz, there is a slight reduction in C_d. Also, at poststall conditions, the actuators operating at lower frequencies increase C_d, whereas the actuators operating at 900 Hz cause no change in C_d.

From the lift and drag results, it is evident that the actuators have a beneficial effect on both C_ℓ and C_d. But the results also suggest that both the Re_N and the frequency of the actuators affect C_ℓ and C_d too. No considerable benefits could be achieved by either increasing C_ℓ or reducing C_d without improving the lift-to-drag ratio (C_ℓ/C_d) of the aerofoil. Therefore, it becomes essential to increase C_ℓ and C_ℓ/C_d by reducing C_d of the aerofoil. To examine the effect of the actuators on

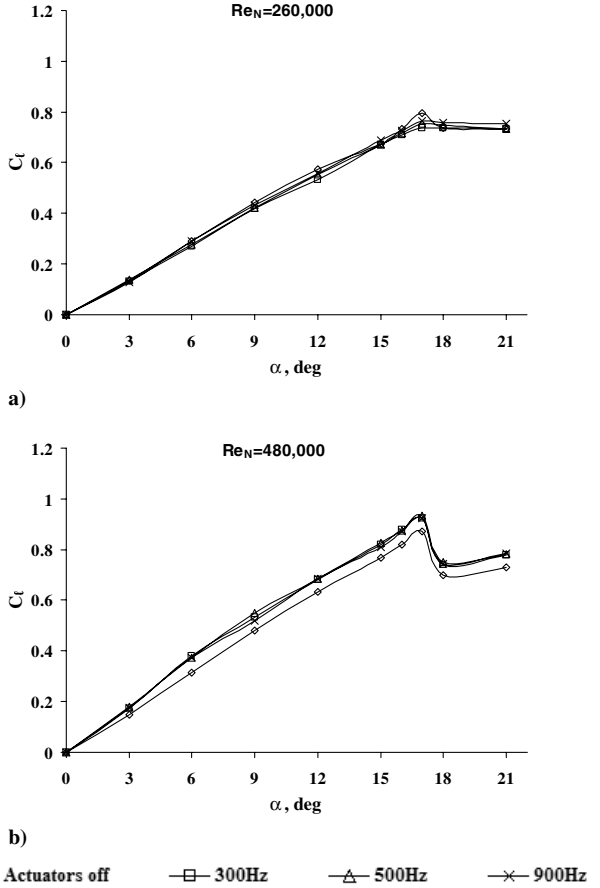

Fig. 4 Effect of the actuator frequency on the C_ℓ (actuators operating at 0.25c).

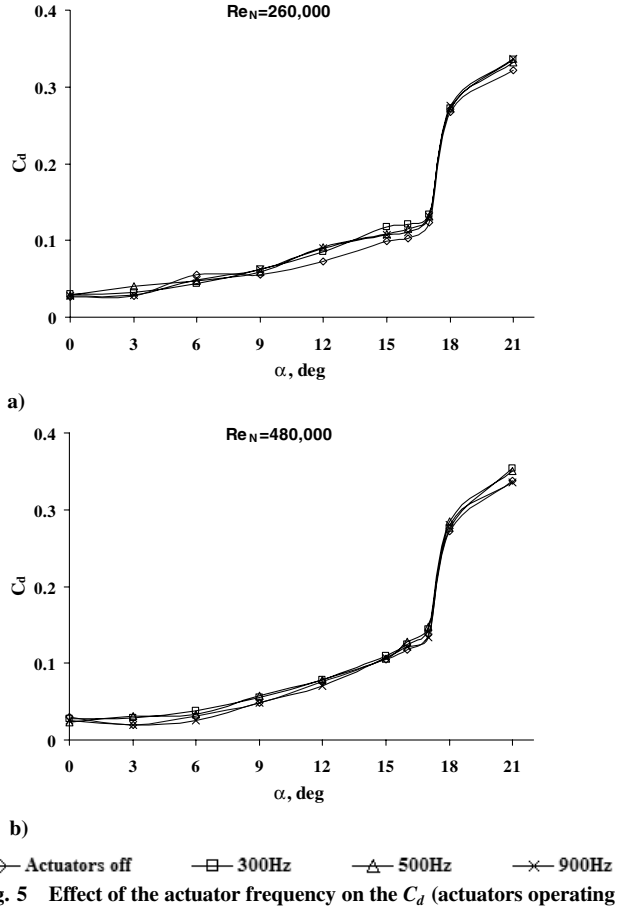

Fig. 5 Effect of the actuator frequency on the C_d (actuators operating at 0.25c).

C_ℓ/C_d of the aerofoil, comparisons were made between the actuators off and on conditions. The values of C_ℓ/C_d were determined from the lift and drag results and these are shown in Fig. 6.

It can be seen in Fig. 6a that the actuators have a negative effect on the lift-to-drag ratio of the aerofoil. This effect is because of the increased drag, Fig. 5a, due to the actuators operating at a low Re_N. However, at a high Re_N, the actuators seem to have a positive effect on C_ℓ/C_d. Also, C_ℓ/C_d increases with increasing actuator frequency. This is because of the lower drag produced, Fig. 5b, with the actuators operating at 900 Hz. The maximum lift-to-drag ratio of the aerofoil increases from 6.8 to 14 at this frequency of operation. This gives an overall increment of 47% in the maximum lift-to-drag ratio of the aerofoil.

2. *Actuators Operating at* 0.5c

For this case, the actuators located at 0.25c were switched off, and those located at 0.5c were electrically simulated and the force measurements were repeated.

Figure 7 indicates that the actuators operating at 0.5c show similar trends to those operating at 0.25c. At a low Re_N, Fig. 7a, C_ℓ is unaffected due to the actuators, and only a slight reduction in C_ℓ is notable between 7 and 11 deg angles of attack at 900 Hz. At a high Re_N, an increment in C_ℓ is observed for all incidences, Fig. 7b. $C_{\ell\,\max}$ is considerably increased, and the highest effect seems to occur at a frequency of 300 Hz. Therefore, as seen previously with the actuators operating at 0.25c, the Re_N seems to play an important role. The actuators are ineffective at a low Re_N, whereas they tend to increase C_ℓ as the Re_N increases. The effect of altering the frequency, however, does not follow any notable trend. At a high Re_N, the lower frequencies produce a higher value of C_ℓ, but the variations in C_ℓ caused due to the change in the actuator operating frequency are, in fact, small.

Figure 8 shows that with the piezoelectric actuators operating at 0.5c, C_d increases at both a low and a high Re_N. In the previous case (0.25c), however, a reduction in C_d was observed at high a Re_N for the actuators operating at 900 Hz. Even though the aerofoil produces more lift at both a low and a high Re_N, the increased drag due to the actuators will obviously have a negative effect on C_ℓ/C_d.

As with the 0.25c case, the values of C_ℓ/C_d were determined from the lift and drag results, and these are shown in Fig. 9. As expected, the results for C_ℓ/C_d with the actuators operating at 0.5c show no increment. At a low Re_N, due to the increased drag and no change in lift, the lift-to-drag ratio is reduced significantly. At a high Re_N, both the lift and drag increase for all of the frequencies tested.

It is important to note that the interpretation of the force measurements should be done with caution and in conjunction with the boundary-layer surveys presented in Sec. III.B. There are experimental errors associated with mounting the force balance on top of the wind-tunnel section. The three-component force balance used in the present experiments is ideally suited for models placed horizontally inside the wind tunnel. However, the weight of the aerofoil was too large and, as a result, the model was placed vertically inside the wind tunnel with the force balanced fitted horizontally on top of the wind-tunnel test section. At that mounting, even though adjustments were made to bring the force balance close to its original reference point, the direction of the measurement may deviate slightly, which produces errors in the force measurements. Another possible source of error could be due to a contact between the force balance and the top section of the test section.

From the force measurement results, it was found that at a Re_N of 280,000, the actuators had either no effect or a slightly negative effect on C_ℓ. At a Re_N of 480,000, the actuators had the maximum beneficial effect on C_ℓ and C_ℓ/C_d. Also, it was found that at a frequency of 900 Hz, the piezoelectric actuators were the most effective in terms of improving the lift-to-drag ratio. Therefore, the remaining experiments were performed at these two different Re_N and at a frequency of 900 Hz. In the following sections, a low Re_N corresponds to a value of 280,000 and a high Re_N corresponds to a value of 480,000.

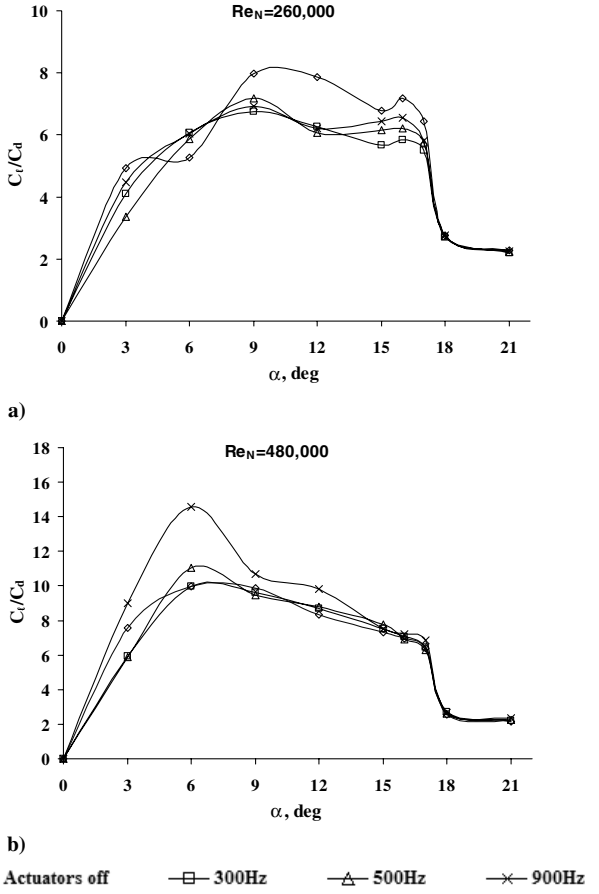

Fig. 6 Effect of the actuator frequency on the C_ℓ/C_d (actuators operating at 0.25c).

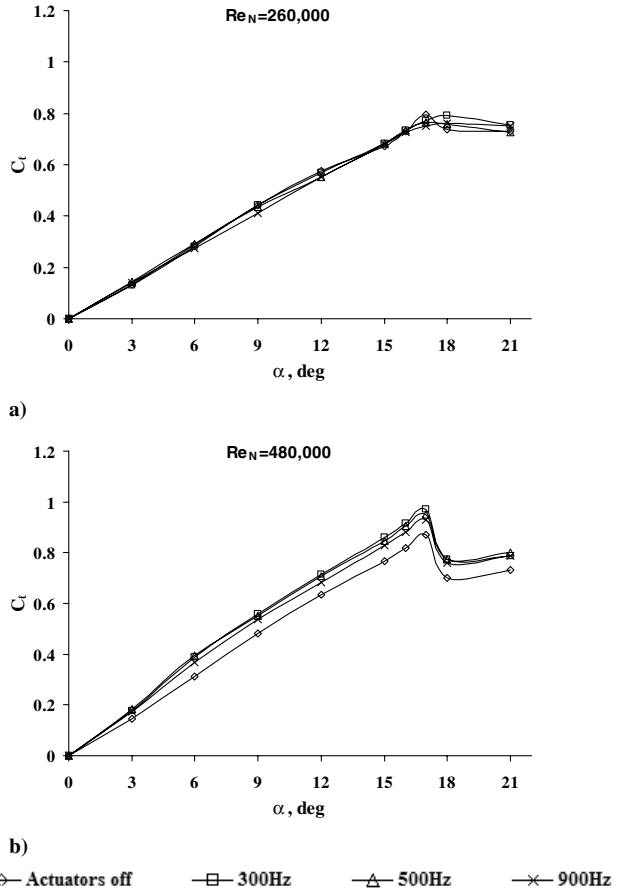

Fig. 7 Effect of the actuator frequency on the C_ℓ (actuators operating at 0.5c).

B. Boundary-Layer Measurements

It is important to note that the small aspect ratio (less than 2) of the NACA 0015 aerofoil model used in this research, the large pressure gradients involved, and the discrete spanwise nature of the actuators strongly suggest the presence of major spanwise effects. Also, given the low Reynolds number of the study, the following classes of physical effects are present or expected along with their interactions: 1) an attached flow transition, 2) a separated flow/shear layer transition, 3) driven quasi-organized longitudinal and transverse vortical flow dynamics in both attached and separated flows, and 4) Parker mode standing nonlinear acoustic waves. All of these flow phenomena and their interactions probably have extensive spanwise variability/3-D flow behavior. However, the work undertaken in the current research only deals with the 2-D flow behavior and, as a result, only longitudinal profile measurements have been taken.

A detailed boundary-layer investigation was carried out to examine the effect of the actuators on the mean velocity and turbulence intensity profiles. The boundary-layer thickness, δ, was also determined at each location, and the results were compared for the actuators on and off conditions. Measurements were taken along the midchord of the aerofoil at 1) $x/c = 0.15, 0.25, 0.35, 0.55, 0.75$, and 0.95; 2) angles of attack of 0, 6, 12, 15, and 18 deg; 3) a low and a high Re_N; and 4) an actuator frequency of 900 Hz with actuators placed at 0.25 and 0.5c.

A conventional single hot-wire probe was used for the boundary-layer measurements. It is important to note that a conventional hot-wire probe cannot distinguish the direction of the flow due to the directional symmetry of the wire element. As a consequence, measurements with such a probe in separated flows, displaying regions with reverse flow, will give erroneous results. One such flow case that has been extensively studied both experimentally and numerically over the past decades is the laminar separation bubble flow caused by an adverse pressure gradient. The insensitivity of the single hot wire to the direction of the flow, for example, in the laminar separation bubble gives erroneous measurements of the mean and the rms of the streamwise velocity in the low velocity region close to the wall where reverse flow occurs. In transition experiments in which the evolution in the separation bubble of different types of artificially generated deterministic disturbances is studied, the directional insensitivity will lead to an uncertainty of the behavior and structure of these disturbances.

1. *Low Re_N*

Figure 10 shows the effects of the actuators operating at 900 Hz on δ. Comparisons have been made between the actuators operating at 0.25 and 0.5c. The boundary-layer thickness profiles in Fig. 10 show that the actuators operating at 900 Hz are ineffective at low incidences. The actuators located at both 0.25 and 0.5c produce no significant changes in δ. Even at a 12 deg incidence, no major effect due to the actuators is seen in Fig. 10. However, at 15 deg, δ decreases drastically with the actuators operating at 0.25c. The changes take place at the location where the actuators are placed (i.e., at $x/c = 0.25$). Downstream of this location, δ continues to be lower than that measured for the actuators off condition. Even though the reduction in δ reduces in magnitude toward the trailing edge, the effect of the actuators on δ is evident across the aerofoil's chord. At $x/c = 0.15$, no changes in δ are seen due to the actuators operating at 0.25c. This suggests that the actuators produce changes in the boundary layer downstream of their location. Examining the δ profiles for the actuators at 0.5c, a similar trend is observed. The boundary-layer thickness reduces from $x/c = 0.6$ onward, indicating that changes take place only downstream of the location of the actuators. In the case of the actuators operating at 0.5c, the effect is, however, smaller than that observed with the 0.25c case. At poststall conditions, that is, at 18 deg, the actuators operating at 0.5c produce no change at all in δ. However, with the actuators operating at 0.25c, a reduction in δ is observed between $x/c = 0.4$ and 0.8.

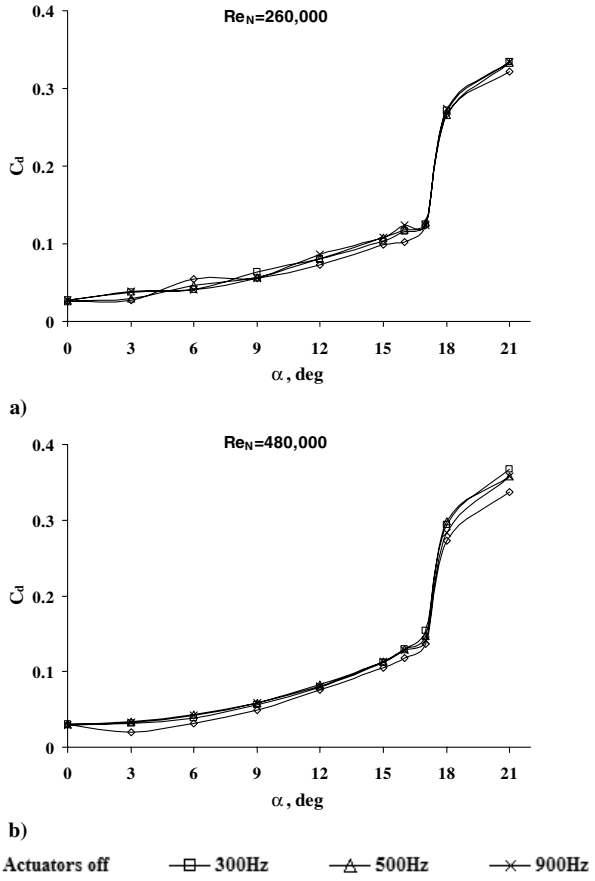

Fig. 8 Effect of the actuator frequency on the C_d (actuators operating at 0.5*c*).

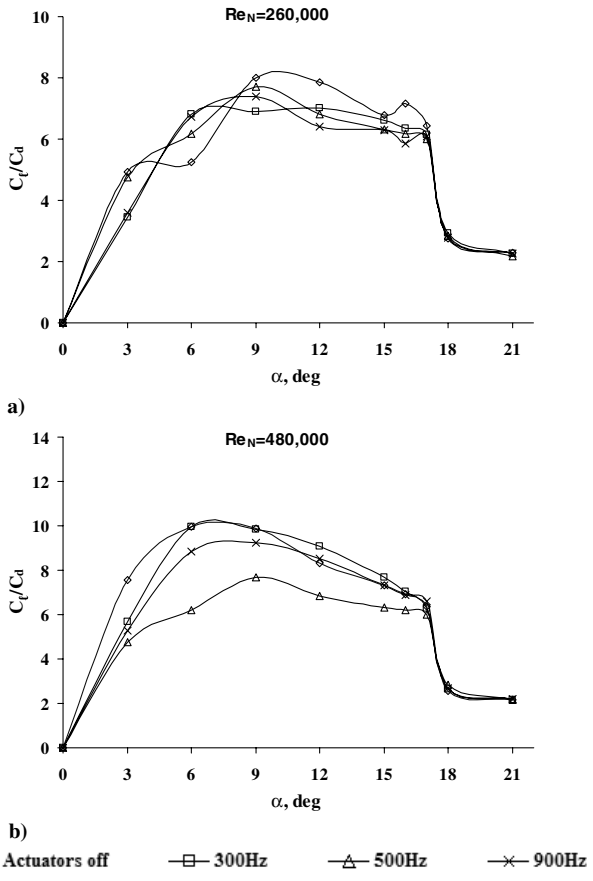

Fig. 9 Effect of the actuator frequency on the C_ℓ/C_d, (actuators operating at 0.5*c*).

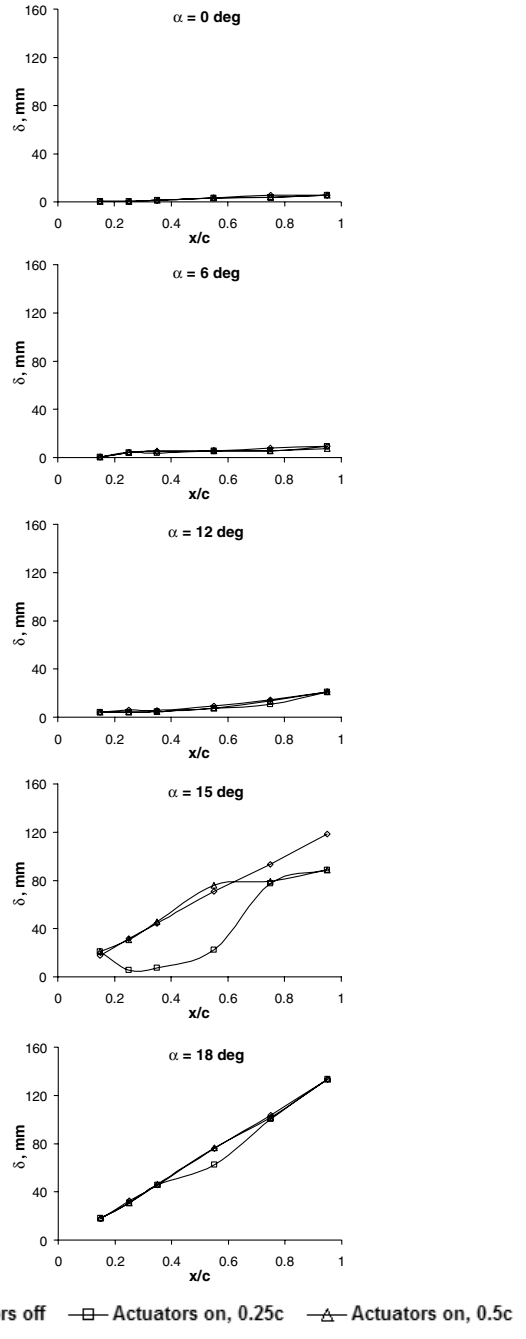

Fig. 10 Effects of the operating actuators on δ at a Re_N of 280,000.

The mean velocity profiles at $\alpha = 15$ deg and at a low Re_N of 280,000 are shown in Fig. 11. The profiles show that, upstream of the location of the actuators, the flow seems to be only slightly affected due to the actuators operating at 900 Hz. Compared with the actuators off condition, the flow seems to have gained momentum. However, this effect is only seen until $y/\delta = 0.6$. This means that, upstream of their location, the actuators affect the flow velocity just about halfway within the boundary layer. When the actuators operate at $0.25c$, a drastic increase in flow velocity is evident at $x/c = 0.25$. Because of the actuators operating at such a high frequency, the velocity near the wall significantly increases and continues to grow within the boundary layer. Downstream of this location, an increased effect in flow velocity is still seen at $x/c = 0.35$. This effect is then reversed downstream of this location. At $x/c = 0.55$, the flow velocity reduces near the wall and continues to lose momentum until $y/\delta = 0.4$. Further downstream, the flow velocity near the wall increases, but the effect is reversed from $y/\delta = 0.38$ onward. Beyond this point within the boundary layer, the flow loses momentum due to

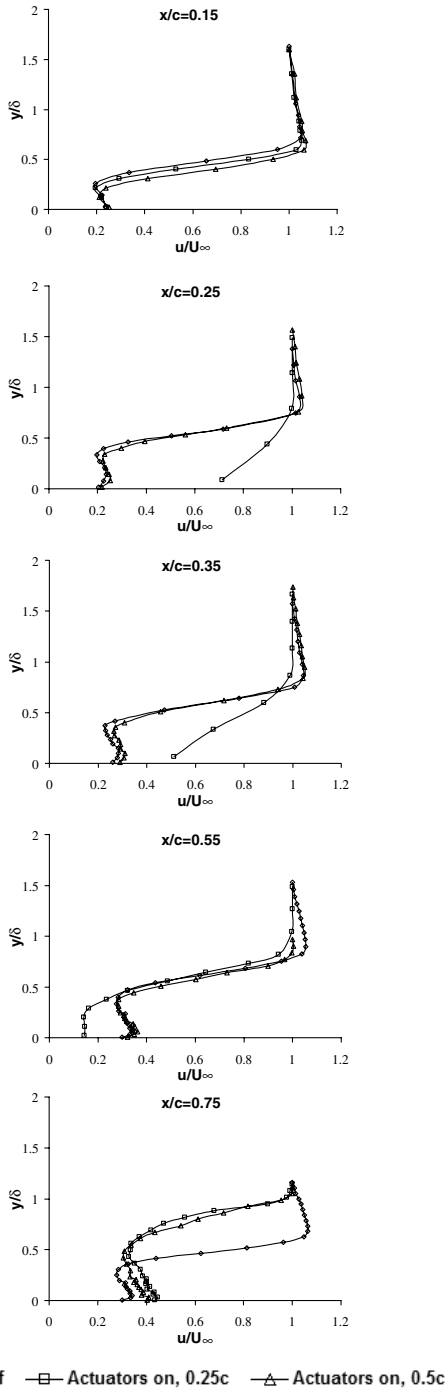

Fig. 11 Effects of the operating actuators on the mean velocity profiles at $\alpha = 15$ deg and a Re_N of 280,000.

the actuators operating at $0.25c$. However, when the actuators operate at $0.5c$, significant effects are only seen further downstream of their location, that is, at $x/c = 0.75$. At this location, the flow behaves exactly the same way as that of the actuators operating at $0.25c$. Just downstream and upstream of their location, only a slight increase in the flow velocity near the wall region is seen at $x/c = 0.35$ and 0.55.

The mean velocity profiles in Fig. 11 show that the flow is separated at all locations when the actuators are off. When the actuators are switched on at $0.5c$, the flow still remains separated. However, when the actuators are switched on at $0.25c$, the flow becomes attached from between $x/c = 0.25$ and 0.35. Upstream of $x/c = 0.25$, the actuators have no effect, and the flow remains separated. Similarly, far downstream (i.e., at $x/c = 0.55$ onward), the effects of the actuators are minimized. As explained in Sec. III.B, a detailed description and discussion of the hot-wire measurement is inappropriate as the reverse flow cannot be measured with the current hot-wire anemometry system.

One important feature in a separated region is that, at the edge of the separated boundary layer, where the velocities change direction, a line of vortices occur (known as a vortex sheet). This happens because fluid to either side is moving in the opposite direction. However, the velocity profiles shown in Fig. 11 fail to show the change in direction. This is because of the limitations of the hot-wire probe in a reversing flow.

Figure 12 shows the turbulence intensity profiles at $\alpha = 15$ deg and at a low Re_N of 280,000. The reduction in the turbulence intensity in Fig. 12 due to the actuators operating at $0.25c$ is clearly evident at $x/c = 0.25$ and 0.35. The reduction is only seen behind the location of the actuators. Downstream of $x/c = 0.35$, the turbulence intensity slightly increases but only up to halfway within the boundary layer. Beyond this point, the turbulence intensity seems to be unaffected. No significant changes in the turbulence levels, either upstream or downstream, are seen with the actuators operating at $0.5c$. Further downstream, that is, at $x/c = 0.75$, the turbulence seems to be unaffected up to halfway within the boundary layer. An increase in turbulence levels is then evident from $y/\delta = 0.6$ and 0.5 for the actuators operating at 0.25 and $0.5c$, respectively.

2. *High Re_N*

Examining the δ profiles in Fig. 13, it can be seen that the boundary-layer thickness remains mostly unchanged at lower incidences. Significant changes are only observed at higher incidences. When the actuators operate at $0.25c$, δ increases from $x/c = 0.25$ onward until $x/c = 0.6$. This effect is then reversed from $x/c = 0.6$ onward, and δ actually reduces when compared with the actuators off condition. As seen previously (at a low Re_N), the actuators alter the boundary layer downstream of their location only. Upstream of their location, no changes are observed. The same effect is also seen in Fig. 13. When the actuators operate at $0.5c$, similar effects are seen. In this case, the increase in δ, as expected, occurs from $x/c = 0.5$ until $x/c = 0.7$. δ then reduces downstream of this location when compared with the actuators off condition. Once again, comparing the two cases, it can be seen that changes in δ are greater for the actuators operating at $0.25c$ than those operating at $0.5c$. At an 18 deg incidence, δ seems to be unaffected due to the operation of the actuators but only until $x/c = 0.35$. For the actuators operating at $0.25c$, δ seems to grow compared with the actuators off condition. For the actuators operating at $0.5c$, δ reduces upstream of their location. At $x/c = 0.7$, this effect is reversed and δ increases only slightly when compared with the actuators off condition.

Figure 14 shows the mean velocity profiles at $\alpha = 15$ deg and at a Re_N of 480,000. With the actuators operating at $0.25c$, the effect of increased momentum is seen at $x/c = 0.25$. The flow velocity near the wall region increases and continues to be higher within the boundary layer. At $x/c = 0.35$, the near wall region of the flow remains unaffected, but the flow then gains momentum and becomes more turbulent. At $x/c = 0.55$, the velocity profile remains largely unaffected. However, at $x/c = 0.75$, the flow velocity in the near wall region now decreases and continues to be lower within the boundary layer. The results therefore show that, upstream of the location of the actuators, the velocity profiles are unaffected as seen at $x/c = 0.15$. At locations downstream of the actuators, the flow gains momentum, but further downstream this effect is reversed and the flow actually slows down. The actuators operating at $0.25c$ are most effective between $x/c = 0.25$ and 0.55. When the actuators operate at $0.5c$, a reduction in the flow velocity near the wall region is seen upstream of their location at $x/c = 0.15$. At $x/c = 0.25$, the flow seems to be mostly unaffected. However, at $x/c = 0.35$, the flow reduces momentum in the near wall region. The profile becomes more laminar in this case, as seen at $x/c = 0.35$. Further downstream of this location, the flow behaves the same way as it does for the $0.25c$ case. The most significant changes in the velocity profiles for both the cases are, therefore, seen at $x/c = 0.35$.

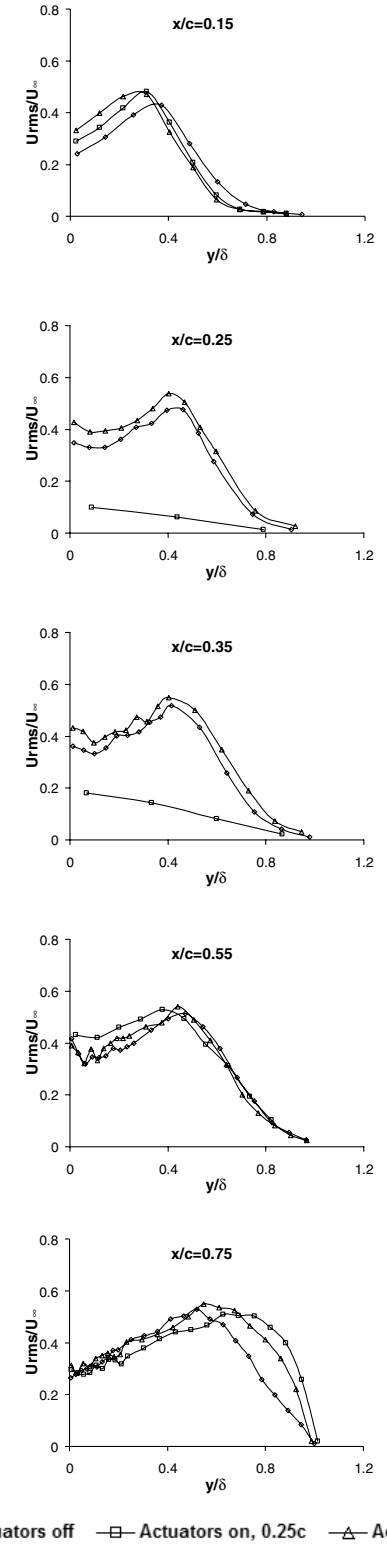

Fig. 12 Effects of the operating actuators on the turbulence intensity profiles at $\alpha = 15$ deg and a Re_N of 280,000.

Figure 15 shows the turbulence intensity profiles at $\alpha = 15$ deg and at a Re_N of 480,000. The profiles show no significant changes in turbulence levels at either $x/c = 0.15$ or 0.25. However, at $x/c = 0.35$, with the actuators operating at $0.25c$, the turbulence levels are reduced. For the $0.5c$ case, the turbulence levels actually increase compared with the actuators off condition. Opposite effects in velocity profiles at this location were also observed in Fig. 14. At $x/c = 0.55$, the near wall region remains unaffected for both cases, but the turbulence levels start to reduce from $y/\delta = 0.4$ onward.

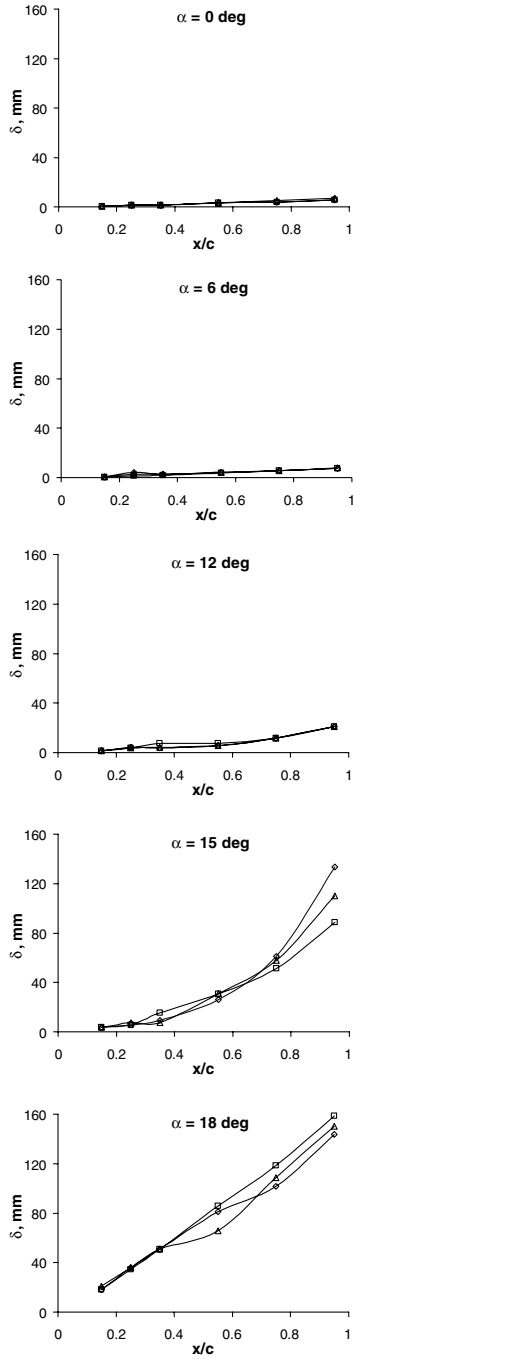

Fig. 13 Effects of the operating actuators on δ at a Re_N of 480,000.

However, at $x/c = 0.75$, reverse effects are observed from $y/\delta = 0.4$ onward. The turbulence levels increase due to the actuators operating at both 0.25 and $0.5c$.

To make a more quantitative assessment on the relative merits of piezoelectric actuators operating at different chordwise positions, the distributions of the boundary-layer integral parameters, namely the boundary-layer displacement thickness, δ^*; the momentum thickness, θ; and the shape factor, H, have been examined. The effects of oscillation on these parameters will shed light onto the mechanisms associated with a reduction in skin-friction drag. The parameters are defined as follows [25,26]:

$$\delta^* = \int_0^{\delta} \left(1 - \frac{u}{U_0}\right) \mathrm{d}y$$

where δ^* is the boundary-layer displacement thickness, u is the local velocity, U_0 is the velocity at the edge of the boundary layer, and y is

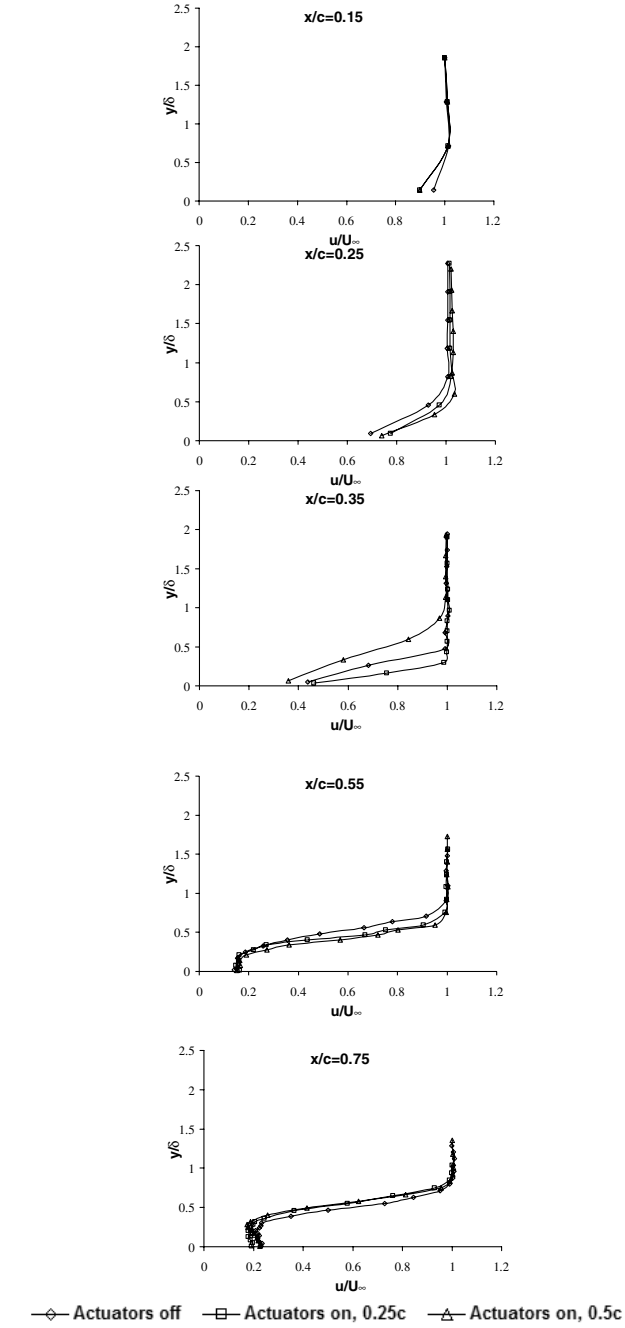

Fig. 14 Effects of the operating actuators on the mean velocity profiles at $\alpha = 15$ deg and a Re_N of 480,000.

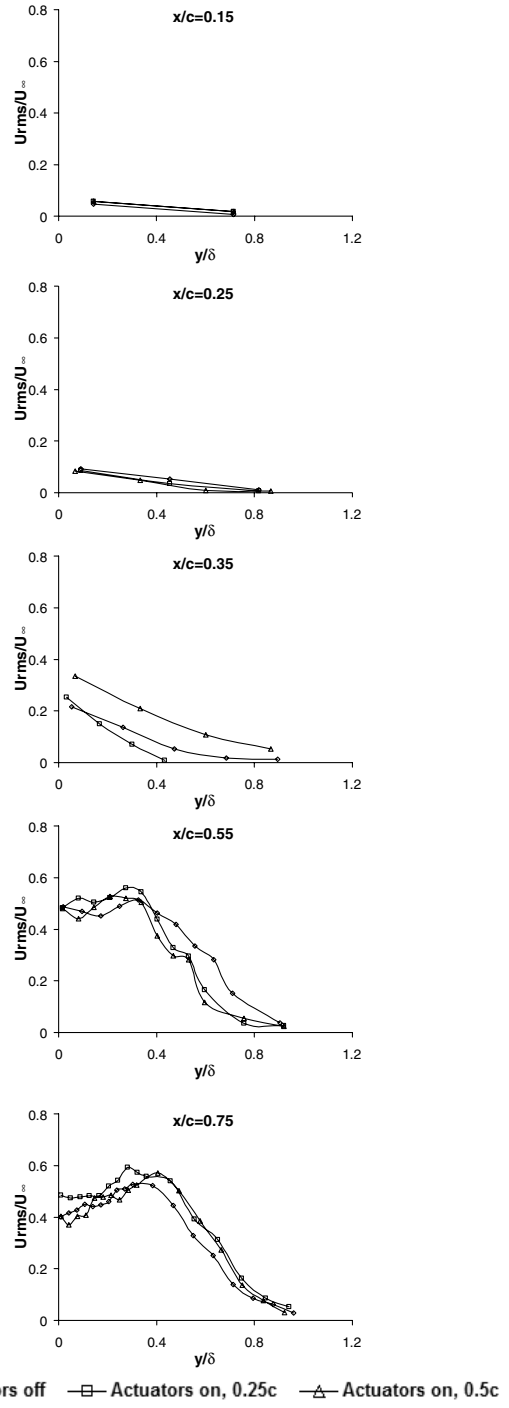

Fig. 15 Effects of the operating actuators on the turbulence intensity profiles at $\alpha = 15$ deg and a Re_N of 480,000.

the displacement from the surface. θ is the momentum thickness, given by

$$\theta = \int_0^\delta \frac{u}{U_0}\left(1 - \frac{u}{U_0}\right) \mathrm{d}y$$

The shape factor, H, is given by

$$H = \frac{\delta^*}{\theta}$$

The displacement thickness is an indicator of how much the external inviscid flow is deflected by the viscous boundary layer, with adverse pressure gradients and separation causing an increase in δ^*. Further, separation is known to occur [27,28] when $2 < H < 2.8$, so that we can assess how far the flow is removed from the incipient separation condition.

Figure 16 shows the effect of the actuators on the boundary-layer properties at a Re_N of 280,000 and at an incidence of 15 deg. Figure 16a shows that, with the actuators off, the displacement thickness increases across the midchord of the aerofoil. When the actuators are switched on at $0.25c$, δ^* reduces drastically. Significant reductions are seen up to a distance of $x/c = 0.55$. Downstream of this location, δ^* increases steeply and, at $x/c = 0.7$, the value of δ^* is the same as that for the actuators off condition. The large decrease in δ^* observed in Fig. 16a suggests the suppression of separation. The suppression of separation will increase lift. However, according to Fig. 7a, no major differences are observed between the actuator off and on cases. As explained in Sec. III.A.2, the discrepancy is attributed to experimental errors associated mainly with the mounting of the balance.

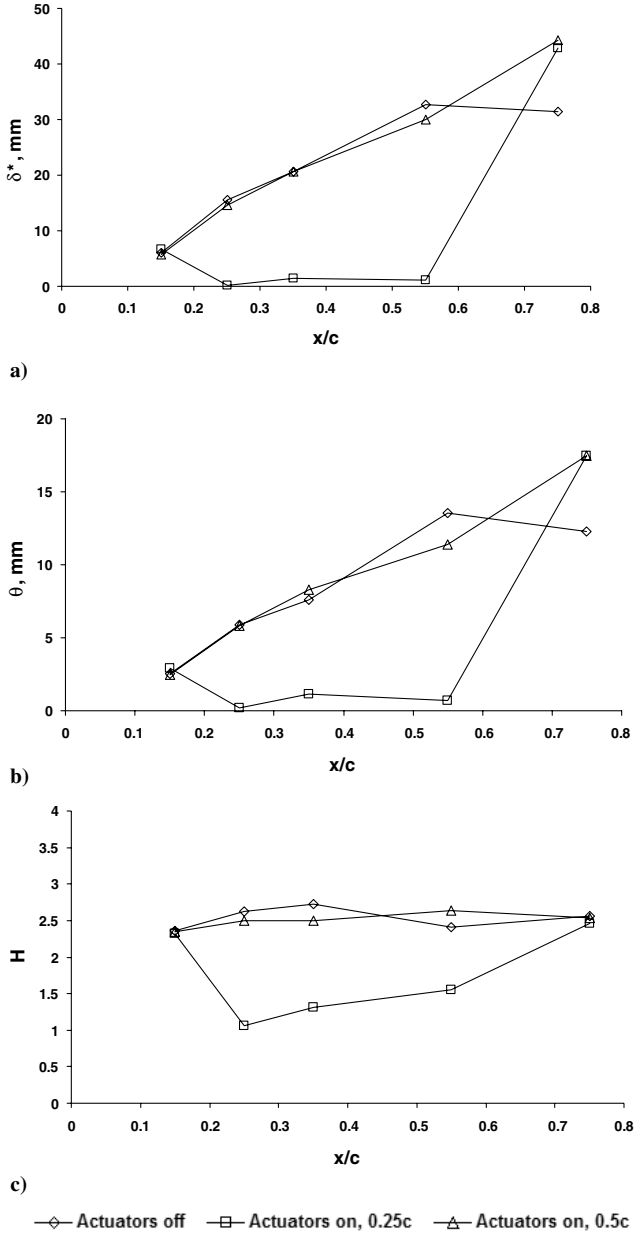

Fig. 16 Effects of the actuators at $Re_N = 280,000$ and $\alpha = 15$ deg: a) displacement thickness, b) momentum thickness, and c) shape factor.

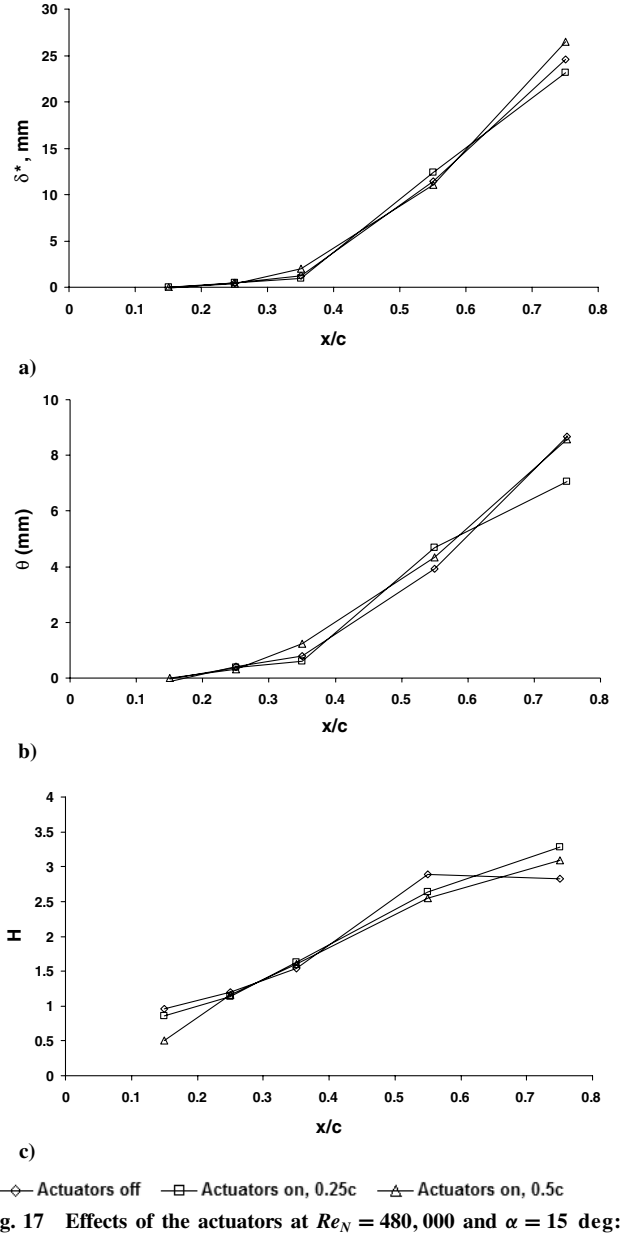

Fig. 17 Effects of the actuators at $Re_N = 480,000$ and $\alpha = 15$ deg: a) displacement thickness, b) momentum thickness, and c) shape factor.

When the actuators operate at $0.5c$, as expected, δ^* remains mostly unaffected. An increase in δ^* is noted downstream of the location of the actuators. These results correlate with those previously shown in Fig. 10. A similar trend can be also seen in Fig. 16b, in which the value of the momentum thickness reduces with the actuators operating at $0.25c$, but no such changes are observed when the actuators are operating at $0.5c$.

It is interesting to note that both the δ^* and θ reduce to a value close to zero between $x/c = 0.25$ and 0.55. This is because the actuators make the boundary layer thinner between these two locations as previously seen in Fig. 10. As a result, the graphs in Figs. 16a and 16b are seen almost touching the x axis. The shape factor profiles in Fig. 16c show that, when the actuators are switched off, the flow is separated across at all of the measured locations, because the value of H is greater than 2. When the actuators are switched on at $0.25c$, a reduction in the value of H from $x/c = 0.25$ onward suggest the flow is no longer separated. The reduced value of H is observed until $x/c = 0.68$. The actuators operating at $0.25c$, therefore, eliminate the flow separation and in the downstream direction only. Upstream of their location, the flow still remains separated, as shown by an increased value of H (i.e., greater than 2). However, when the actuators are operating at $0.5c$, the value of H remains mostly unchanged and this shows that the flow remains separated across the entire aerofoil.

The effects of the actuators on different boundary-layer properties at a Re_N of 480,000 are shown in Fig. 17. Examining the profiles for δ^* in Fig. 17a, it can be seen that the actuators have no effect at all either at 0.25 or $0.5c$. δ^* remains mostly unchanged across the aerofoil at all of the measured locations. These results correlate with the graphs shown in Fig. 13, in which δ remained unaffected. Even though θ profiles in Fig. 17b show slight changes in the momentum thickness when the actuators operate at $0.25c$, the actual difference between the values is small and this could be due to experimental uncertainties. The shape factor profiles show no significant reduction in the values of H with the actuators operating at either 0.25 or $0.5c$. When the actuators are off, the flow becomes separated at $x/c = 0.45$ onward, as seen in Fig. 17c. With the actuators operating, the flow still remains separated at these locations. The results, therefore, show that the actuators in this case do not eliminate separation. However, reduced values of H downstream of $x/c = 0.42$ show that separation is slightly delayed with the actuators on.

The boundary-layer results, therefore, confirm the findings from the force measurements. The actuators operating at $0.25c$ seem to be

more effective than those operating at $0.5c$. The effect of the Re_N is evident on the boundary-layer development in the presence of the actuators. Significant changes in the boundary layer are seen only at higher angles of attack and mainly downstream of the location of the actuators. It is conjectured that two different roles can be determined from the boundary-layer measurements: 1) the actuators simply act as turbulators, and 2) the actuators actively interact with the boundary layer and the flowfield itself. They generate periodic vortices in a separating flow at or near an optimal frequency. Vortices formed at this frequency exhibit high streamwise momentum and are driven toward the surface, energizing the boundary layer and thus eliminating massive separation. At a low Re_N, the piezoelectric actuators were able to produce significant flow disturbances in the boundary layer. This effect was minimized at a higher Re_N. This is because, despite the production of significant perturbations, the actuators' displacement falls well below that required by most microvortex systems in which the displacements range from 2 to 10 mm. Also, compared with oscillatory blowing and synthetic jets, which require actuation jet velocities around the same order of magnitude as the freestream velocity [29], the typical induced velocities of actuators are much lower. Therefore, the interaction is minimized when the freestream velocity increases (and, therefore, the Re_N). It is believed that the physical phenomenon associated with this active flow control mechanism is very similar to that observed by Mangla and Sinha [20]. They found that the vibrations of a very small amplitude could introduce small fluctuations at the location of zero pressure gradient on the suction side of the aerofoil. Any disturbance in the pressure gradient introduced at this point directly induced disturbances in the freestream. This perturbation, when reinforced by a second similar perturbation or at least not nullified by similar perturbations introduced in the vicinity, gets convected to the separated shear layer. This introduces disturbances in the separated shear layer near the point of separation. The enhanced mixing at this point causes the reattachment of the separated shear layer and makes the zero pressure-gradient point on the suction side move downstream.

The results from both the force measurements and the boundary-layer profiles strongly suggest the likely existence of laminar separation bubbles. These are certainly an important flow structure associated with the actuators. The location of the actuators influences the boundary layer, and the results suggest that if the laminar separation line occurs downstream of the actuators, then they have little effect. If the separation line occurs upstream, then the actuators break up the bubble and eliminate its influence on the flowfield. At higher Reynolds numbers, the actuators act as though their influence is such that they effectively exceed the critical roughness height and, at lower Reynolds number, they do not.

IV. Conclusions

The effects of piezoelectric actuators at two chordwise positions on a NACA 0015 aerofoil were examined. The results from the force measurements suggest that, by increasing the Re_N, the actuators operating at both 0.25 and $0.5c$ increase lift. The drag force also increases for actuators operating at lower frequencies. However, for the actuators operating at a higher frequency of 900 Hz, the reduction in drag is observed at a high Re_N. This increases the overall lift-to-drag ratio of the aerofoil. The force measurements, therefore, show that the actuators operating at $0.25c$ are more effective than those operating at $0.5c$. An increment of 47% in the maximum lift-to-drag ratio was observed with the actuators operating at a frequency of 900 Hz.

The boundary-layer measurements show that the actuators are ineffective at lower incidences. At incidences greater than 12 deg, significant changes in the mean velocity and turbulence intensity profiles were observed. Changes in the boundary-layer thickness were also observed at higher angles of attack. The mean velocity and turbulence intensity profiles at 15 deg show that the actuators operating at $0.25c$ are more effective in altering the boundary layer than those operating at $0.5c$. They do so by increasing the flow momentum and reducing the turbulence intensity downstream of their location, thus reducing the boundary-layer thickness at these locations. However, no significant changes either in the velocity profiles or turbulence intensity profiles were seen with the actuators operating at $0.5c$.

The boundary-layer properties with the actuators operating at $0.25c$ have shown that separation could be eliminated at a Re_N of 280,000. The flow becomes attached at the location of the actuators and up to a certain distance in the downstream direction. Upstream of their location, the flow still remains separated. With the actuators operating at $0.5c$, the flow remains fully separated across the entire aerofoil. Even though the actuators do not eliminate separation at a Re_N of 480,000, a reduced value of the shape factor suggests that separation is slightly delayed. The results from both the force and boundary-layer measurements show that, at a Re_N of 480,000, the actuators operating at $0.25c$ and at 900 Hz give the maximum output of the overall piezoelectric actuator system.

Two separate roles of the actuators have also been identified from the boundary-layer measurements. The actuators act as turbulators and they also either eliminate or delay separation at low Reynolds numbers. When electrically stimulated, it is believed that the actuators interact directly with the flowfield. This flow control mechanism generates periodic vortices in a separating flow at or near an optimal actuator frequency. Vortices formed at this frequency exhibit high streamwise momentum and are driven toward the surface, energizing the boundary layer and thus eliminating massive separation.

The results from this research clearly show that the actuators have the potential of increasing lift, and they could be used for either delaying or eliminating separation. However, the complete structure of the flow in the boundary layer near the wall region is difficult to understand from the present measurements. Therefore, investigations are now being performed both numerically and experimentally using computational fluid dynamics and particle image velocimetry. The results from these studies would enhance our understanding of the physical mechanisms associated with the operation of actuators.

Acknowledgments

The authors would like to thank Shota Miyoshi for his assistance in the investigation and ORS-UK for their financial support.

References

[1] Schlichting, H. T., *Boundary Layer Theory*, McGraw–Hill Series in Mechanical Engineering, McGraw–Hill, New York, 1979.

[2] Gad-el-Hak, M., and Bushnell, D., "Separation Control: Review," *Journal of Fluids Engineering*, Vol. 113, No. 1, March 1991, pp. 5–30.

[3] Wiltse, J. M., and Glezer, A., "Manipulation of Free Shear Flows Using Piezoelectric Actuators," *Journal of Fluid Mechanics*, Vol. 249, 1993, pp. 261–270.
doi:10.1017/S002211209300117X

[4] James, R. D., Jacobs, J. V., and Glezer, A., "A Round Turbulent Jet Produced by an Oscillating Diaphragm," *Physics of Fluids*, Vol. 8, No. 9, Sept. 1996, pp. 2484–2495.
doi:10.1063/1.869040

[5] Smith, B. L., and Glezer, A., "The Formation and Evolution of Synthetic Jets," *Physics of Fluids*, Vol. 10, No. 9, Sept. 1998, pp. 2281–2297.
doi:10.1063/1.869828

[6] Bragg, M. B., and Gregorek, G. M., "Experimental Study of Airfoil Performance with Vortex Generators," *Journal of Aircraft*, Vol. 24, No. 5, May 1987, pp. 305–312.

[7] Walsh, M. J., "Drag Characteristics of V-Grooves and Transverse Curvature Riblets," *Viscous Flow Drag Reduction*, edited by G. R. Hough, AIAA, New York, 1980, pp. 168–184.

[8] Gad-el-Hak, M., *The MEMS Handbook*, CRC Press, Boca Raton, FL, 2001.

[9] Kumar, S. M., Reynolds, W. C., and Kenny, T. W., "MEMS Based Actuators for Boundary Layer Control," *Proceedings of the ASME International Mechanical Engineering Congress and Exposition*, American Society of Mechanical Engineers, New York, 1998, pp. 103–109.

[10] Lyle, K. H., and Silcox, R. J., "A Study of Active Trim Panels for Interior Noise Reduction in an Aircraft Fuselage," *Society of*

Automotive Engineers Transactions, Vol. 104, No. 12, 1996, pp. 180–190.

[11] Fuller, C. R., and Silcox, R. J., "Active Structural Acoustic Control," *Journal of the Acoustical Society of America*, Vol. 91, No. 1, Jan. 1992, pp. 519–524. doi:10.1121/1.402743

[12] Fuller, C., and Flotow, A. W., "Control of Aircraft Noise Using Globally Detuned Vibration Absorbers," *Journal of Sound and Vibration*, Vol. 203, No. 5, June 1997, pp. 745–753. doi:10.1006/jsvi.1996.0867

[13] Wehrmann, O. H., "Reduction of Velocity Fluctuations in a Kármán Vortex Street by a Vibrating Cylinder," *Physics of Fluids*, Vol. 8, No. 4, 1965, pp. 760–761. doi:10.1063/1.1761299

[14] Wehrmann, O. H., "The Influence of Vibrations on the Flow Field Behind a Cylinder," Boeing Scientific Research Lab., Document D1-82-0619, 1967.

[15] Wehrmann, O. H., "Self-Adjusting Feedback Loop for Mechanical Systems Influence Flow in Transition. Part I," Boeing Scientific Research Lab., Document D1-82-0632, 1967.

[16] Wiltse, J. M., and Glezer, A., "Manipulation of Free Shear Flows Using Piezoelectric Actuators," *Journal of Fluid Mechanics*, Vol. 249, 1993, pp. 261–285. doi:10.1017/S002211209300117X

[17] Jacobson, S. A., and Reynolds, W. C., "Active Control of Streamwise Vortices and Streaks in Boundary Layers," *Journal of Fluid Mechanics*, Vol. 360, 1998, pp. 179–211. doi:10.1017/S0022112097008562

[18] Mautner, T. S., "Application of Synthetic Jets to Low Reynolds number Biosensor Microfluidic Flows for Enhanced Mixing: A Numerical Study using the Lattice Boltzmann Method," *Proceedings of SPIE: The International Society for Optical Engineering*, Vol. 4937, Nov. 2002, pp. 136–149. doi:10.1117/12.476076

[19] Sinha, S. K., "Aircraft Drag Reduction with Flexible Composite Surface Boundary Layer Control," *2nd AIAA Flow Control Conference*, AIAA, Reston, VA, 2004.

[20] Mangla, N. L., and Sinha, S. K., "Controlling Dynamic Stall Using an Active Flexible Wall," *2nd AIAA Flow Control Conference*, AIAA, Reston, VA, 2004.

[21] Choi, J., Jheon, W. P., and Choi, H., "Control of Flow Around an Airfoil Using Piezoceramic Actuators," *AIAA Journal*, Vol. 40, No. 5, 2002, pp. 1008–1010.

[22] Anon., "Optimization of Synthetic Jet Actuators," NASA Technical Brief LAR-16234, 1995.

[23] Davies, P. G., and Bush, I. J., "Fiber Optic Displacement Sensor," *Fourth Pacific Northwest Fiber Optic Sensor Workshop*, International Society for Optical Engineering, Bellingham, WA, 1998, pp 353–359.

[24] Berthold, J. W., Jeffers, L. A., and Lopushhansky, R. L., "Fiber Optic Sensors for the Refinery of the Future," *Sensors for Industry Conference Houston*, International Society for Optical Engineering, Bellingham, WA, 2002, pp. 202–208.

[25] Garner, H. C., and Rogers, E. W. E., *Subsonic Wind Tunnel Wall Corrections*, North Atlantic Treaty Organization, Brussels, Vol. 109, 1966.

[26] Anon., "Lift Interference and Blockage Corrections for Two-Dimensional Subsonic Flow in Ventilated and Closed Wind Tunnels," Engineering Sciences Data Unit Data Sheet 76028, 1996.

[27] Young, A. D., *Boundary Layers*, Blackwell Science, Boston, 1989.

[28] Schlichting, H., and Gersten, H., *Boundary Layer Theory*, 8th ed., Springer–Verlag, New York, 2000.

[29] Washburn, A. E., Althoff Gorton, S., and Anders, S. G., "Snapshot of Active Flow Control Research at NASA Langley," AIAA Paper 2002-3155, June 2002.